UNIVERSIDADE
DE SÃO PAULO
Instituto de Física de São Carlos

Proceedings of the seminar to the course

Chemical Physics and Thermodynamics of Gases and Solids

SFI5769 / 2024-1

Ph.W. Courteille (editor)
Universidade de São Paulo
Instituto de Física de São Carlos
19/06/2024

.

Contents

Preface

Estes anais (ou proceedings) reúnem as monografias elaboradas pelos alunos do curso de Fundamentos da Interação da Radiação com a Matéria (SFI5905), realizado no Instituto de Física de São Carlos da Universidade de São Paulo durante o primeiro semestre de 2023 sob supervisão do Prof. Ph. W. Courteille.

1

On the Brownian motion according to Einstein

Eduardo V. M. Vieira

Instituto de Física de São Carlos, Universidade de São Paulo, 13560-970 São Carlos, SP, Brazil

Abstract: In this study, we examine Brownian motion from the standpoint of the original paper published by Einstein in 1905. We follow his steps and provide a modern perspective on his approach. Additionally, we briefly cover the topic of the typical stochastic approach and derive the osmotic pressure equation necessary for understanding Einstein's work. Finally, we deduce the diffusion equation and obtain the diffusion coefficient.

1.1 Introduction

The idea of the existence of atoms dates back to ancient Greece and was suggested by philosophers like Democritus and Lucretius, but they were hardly the only ones, the subject entertained the minds of scientists all throughout history. In 1905, during his "miracle year", Albert Einstein published his famous paper on the movement of suspended particles, which was known, though vaguely by him, as Brownian motion [1]. This term refers to the botanist Robert Brown, who about seventy-eight years before, investigated the movement of pollen particles suspended in water. Although his work gained recognition a quantitative analysis had to wait, the mathematical treatment in question, being heavily dependent on the application of Boltzmann's statistical mechanics, which was developed over the subsequent years [8]. In 1908, the chemist and physicist Jean Perrin was capable of verifying experimentally the results obtained by Einstein, along with other fundamental observations about molecules and atoms, for this, Perrin was awarded the Nobel Prize in 1926 [9].

Einstein's work provided strong evidence for the atomic kinetic theory and is historically cited as one of the most important pieces of evidence for the existence of atoms and molecules. Today, matter's atomic (and subatomic) nature is widely accepted as a pillar of modern physics. Brownian motion is now discussed, or at least glossed over, in almost every undergraduate course on physics. However, in contrast to the original thermodynamic approach taken by Einstein, in modern discussions of the problem, the focus is often shifted to the stochastic side of the problem. More specifically, it is treated mathematically as a random walk in conjunction with arguments about the kinetic theory of gases. Of course, this shift is probably done because it makes the subject easier to explain and ties it nicely with the more complete statistical interpretation of thermodynamics. Nevertheless, Einstein's argument still offers an insight into how physics was conducted at the beginning of the last century and the significance of classical thermodynamics in advancing the field. Einstein used the existing knowledge, employing the kinetic theory of heat to derive the so-called osmotic pressure, a phenomenon already known at the time. He was able to use this concept to explain the diffusion of tiny particles suspended in a liquid. From this point of view, it could be argued that Einstein's approach is of great pedagogical relevance for graduate students because it encompasses the creative steps required in cutting-edge research. Knowing this, here we will approach the Brownian motion from the perspective of Einstein in his time.

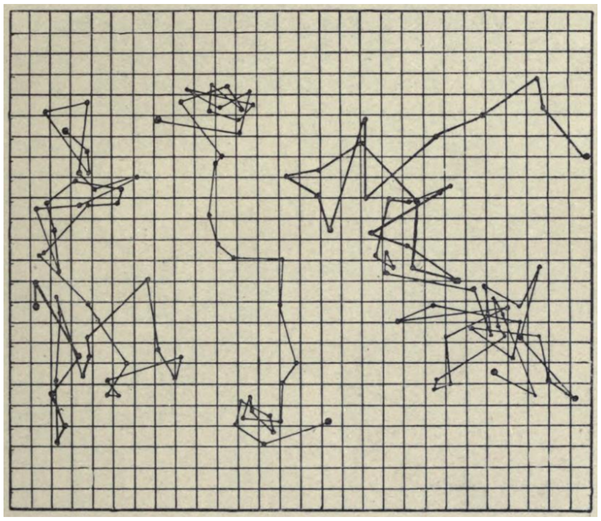

Figure 1.1: A diagram of the bi-dimensional motion of a particle in one of the experiments made by Jean Perrin on the Brownian motion [3]. Each square has approximately 3, 2 μm.

1.2 A simple approach to the one-dimensional Brownian motion

Loosely, the main[1] characteristic of a Brownian motion is that for a random variable X_t, any two consecutive steps $\{X_{t_n} - X_{t_{n-1}}\}$ are mutually independent [5]. Physically we can imagine that a particle experiences collisions with the liquid molecules in which they are suspended, thus the irregular pressure causes them to move around randomly. Their movement should be languid since the particle has an enormous mass compared to the molecules. However, this argument has a nuance that is often ignored, because as stated in reference [2], at first glance, although the movement is expected to be slow, it is much slower than it should be. For example, a particle –say, of pollen– has a mass of the order of 10^{-9} grams [4] and a molecule of water has a mass of the order of 10^{-23} grams. Supposing that the system is in equilibrium, the molecules and the particles should have the same temperature, then by the equipartition theorem, the equation

$$\frac{1}{2}m\langle v^2\rangle = \frac{3}{2}k_B T \tag{1.1}$$

should be valid for both of them. Now, considering that water molecules at ambient temperature are found with an average speed of the order of 10^3 m/s, the expected speed of particles should be of the order of 10^{-4} m/s, that is 0.1 mm/s. But in actuality, the movement is much slower than that, that is, of the order of 0.1 mm/**min** as shown by Perrin [3], he also gives us an explanation which is obvious to us today, i.e., what is being observed is, in reality, an average velocity because as he states about figure 1.1:

> As a matter of fact diagrams of this sort [...] in which a large number of displacements are traced on an arbitrary scale, gives only a very meagre idea of the extraordinary discontinuity of the actual trajectory. For if positions were to be marked at intervals of time 100 times shorter, each segment would be replaced by a polygonal contour relatively just as complicated as the whole figure, and so on.

Mathematically this random motion can be expressed as displacements of the same length ℓ in the x-axis at each time step. Let q be the probability of moving to the right $+\ell$ and $(1-q)$ the probability of moving to the left $(-\ell)$, then for N steps, because the order does not matter, we arrive at the binomial distribution

$$\phi(k, N) = \binom{N}{k} q^k (1-q)^{N-k}. \tag{1.2}$$

Thus, $\phi(k, N)$ expresses the probability that a particle moves k steps to the right and $N - k$ steps to the left[2]. Also, by direct calculation, we obtain the relations:

$$\begin{cases} \langle x\rangle = \sum_{i=1}^{N}\langle x_i\rangle = N\ell(2q-1) \\ \langle x^2\rangle = \sum_{i=1}^{N} x_i^2\phi(x_i, N) = N\ell^2 \\ \sigma^2 = \langle x^2\rangle - \langle x\rangle^2 = 4N\ell^2 q(1-q) \end{cases}. \tag{1.3}$$

Imposing that $p = q = \frac{1}{2}$ we arrive at the average displacement $\langle x\rangle = 0$, of course. Moreover, the mean squared displacement is still $\langle x^2\rangle = N\ell^2$ and, in consequence, the mean square displacement is given by

$$\lambda_x = \sqrt{\langle x^2\rangle} = \sqrt{N}\ell. \tag{1.4}$$

Now, let τ be the average time between collisions starting at the origin, then after N collisions the elapsed time will just be $t = N\tau$. Thus, the mean squared displacement can be rewritten [2] as

$$\lambda_x = \sqrt{2Dt}, \tag{1.5}$$

---

[1] The formal definition [5] also requires that: I) $X(t+s) - X(s)$ follows a normal distribution with $\langle X\rangle = 0$ and variance $\sigma^2 t$, and II) $X(0) = 0$ with $X(t)$ being continuous at t = 0.

[2] Since $x = k\ell - (N-k)\ell$, then $k = \frac{1}{2}\left(N + \frac{x}{\ell}\right)$.

where we introduce the proportionality constant D denominated the *diffusion coefficient*. This number can be used to quantify the diffusion of a gas into another, which is mathematically similar to the Brownian motion of suspended particles. But to obtain an analytic equation for D we will have to wait until section 1.4. Experimentally, though, D can be calculated by projecting the motion of a particle, like in figure 1.1, in one of the axes, e.g., the x-axis.

Of course, what was done until here is discrete, but, we could also use the central limit theorem to show that for $N \to \infty$,

$$\phi(x, N) \approx \frac{1}{\sqrt{4\pi D}} \exp\left(- \frac{x^2}{4\pi D} \right), \tag{1.6}$$

which is an expression a lot easier to deal with.

1.3 Osmotic Pressure

Before introducing the approach taken by Einstein, we need to understand what he proposed to work with, specifically the concept of osmotic pressure. We can start by remembering Gibbs' free energy

$$dG = VdP + SdT + \sum_i \mu_i dn_i. \tag{1.7}$$

So at constant pressure P, temperature T, and number of moles n_j of the j substance, the chemical potential can be defined as

$$\mu_i \equiv \left(\frac{dG}{dN_i} \right)_{T,P,n_{i\neq j}}, \tag{1.8}$$

which is an intensive parameter, thus being independent of the volume of the system. Then,

$$d\mu_i = \bar{V}dP + \bar{S}dT + \sum_i \frac{\partial \mu_i}{\partial N_j} dN_j. \tag{1.9}$$

Finally, for an ideal mixture at *constant temperature*, we find that[3]

$$d\mu_i = \bar{V}_i dP + RTd\ln X_i. \tag{1.10}$$

Now let's suppose that a semipermeable membrane, i.e. that only permits the solvent – e.g. water – to pass through it, divides a volume into two parts like in figure 1.2, each one of them having different concentrations, though very dilute, of a solute –say, kitchen salt–.

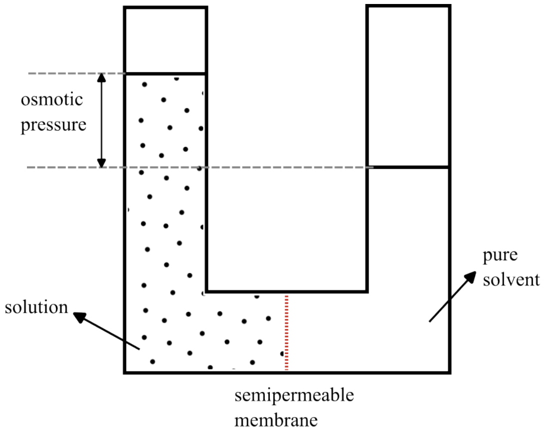

Figure 1.2: Diagram illustrating the osmotic pressure in a U-shaped recipient.

Then in crossing the membrane, there will be a chemical potential gradient [6] given by

$$\mu_i^{(2)} - \mu_i^{(1)} = \bar{V}_i(p_2 - p_1) + RT \ln \frac{X_i^{(2)}}{X_i^{(1)}}. \tag{1.11}$$

In the case when we have a *pure solvent* on one of the sides, the chemical potential on this side will be

$$\mu_1(p_1) = \mu^0 + \bar{V}p_1. \tag{1.12}$$

Along with a *solute* diluted in the same *solvent* (now of molar fraction $0 < X < 1$) on the other, yields the chemical potential

$$\mu_2(p_2) = \mu^0 + \bar{V}p_2 + RT\ln X, \tag{1.13}$$

where p_1 and $p_2 = p_1 + \Pi$ represent the hydrostatic pressures. Here Π precisely indicates the pressure difference caused by the addition of the solute (c.f. figure 1.3). Because the chemical potential of the solution is lower, the pure solvent which has a higher chemical potential, will flow to the side of the solution, and eventually, equilibrium will be reached, that is $\mu_1(p_1) = \mu_2(p_1 + \Pi)$.

In this situation,

$$\bar{V}\Pi = -RT\ln X = -RT\ln(1 - X_s), \tag{1.14}$$

with X_s being the molar fraction of the *solute*. If, as stated earlier, the solution is very dilute we can approximate $\ln(1 - X_s) \approx -X_s$, $X_s \approx n_s/n_l$, $n_l\bar{V} \approx V^*$ where n_s and n_l are the molar quantities of the solute and the solvent, respectively and V^* is the volume of the solution. Thus

$$\Pi = \frac{n_sRT}{V^*}, \tag{1.15}$$

which is the equation Einstein started his work with.

---

[3] For a thermodynamic variable B we define the partial molar quantity by $\bar{B} \equiv \left(\frac{dG}{dn_i}\right)_{T,P,n_j}$. The molar fraction is defined as $X_i \equiv \frac{n_i}{\sum_k n_k}$.'

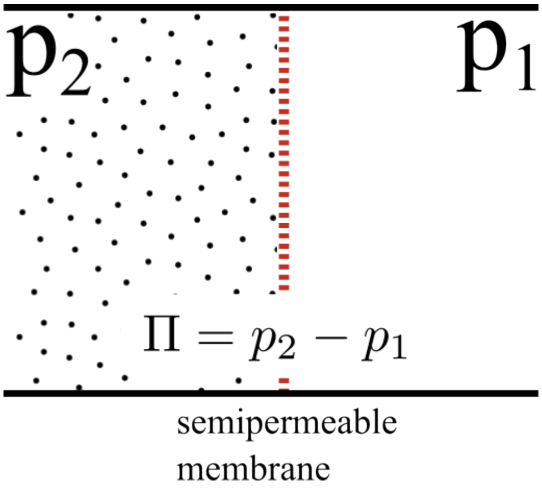

Figure 1.3: Diagram of a close-up of the membrane dividing the two parts of the container.

1.4 Einstein's approach

Einstein [1] had the brilliant realization that the suspended particles should have the same behavior as the dissolved molecules in osmosis and after equilibrium is reached, any semipermeable partition put in this system should reproduce an osmotic pressure of an identical nature to that found in a solution (see figure 1.4). Einstein also notes that classical thermodynamics may not even apply to relatively bigger bodies like the particles visible in a microscope, since, as he argues: the free energy $F = E - TS$ cannot depend on the position of the partition or the particles, so there should not be any force acting on the particles except for gravity, which is not relevant to this analysis.

But in the paradigm of the kinetic theory of heat, the molecules dissolved, when dealing with a solution, and the suspended particles differ only by their masses. So we should be able to see the whole osmosis mechanism described by this theory, which he, then, does next.

1.4.1 Pressure caused by suspended particles

Let $(\vec{r}, \vec{p})$ be state variables of the system, then we can write the free energy as

$$F = -Nk_BT \ln \mathcal{B}, \tag{1.16}$$

with,

$$\mathcal{B} = \int e^{-\beta\epsilon} \mathrm{d}^3\vec{r}\, \mathrm{d}^3\vec{p} \tag{1.17}$$

where ϵ is the element of energy and $\beta = \frac{1}{k_BT}$. For N non-interacting *particles*, the only source of energy is kinetic, hence

$$\begin{aligned} \mathcal{B} &= \int \mathrm{d}^3\vec{r} \int e^{-\beta\epsilon}\, \mathrm{d}^3\vec{p} \\ &= (V^*)^N \left(\frac{2\pi m}{\beta}\right)^{3N/2}, \end{aligned} \tag{1.18}$$

In this case, V^* is meant to represent the volume containing the particles. Consequently,

$$F = -Nk_BT\Big[\ln V^* + \frac{3}{2}\ln\Big(\frac{2\pi m}{\beta}\Big)\Big]. \tag{1.19}$$

Then, at last,

$$P = -\frac{\partial F}{\partial V^*} = \frac{n_sRT}{V^*}. \tag{1.20}$$

The kinetic theory of heat indeed leads to the osmotic pressure. We should note here that this is just the ideal gas equation because although the situation is different, the restrictions we put on these non-interacting particles are equivalent to those of a free ideal gas.

1.4.2 Movement of tiny spherical particles on the surface of a liquid

Since there is a dynamic system at the molecular level, for simplicity, Einstein introduces a force $f(\vec{r})\hat{x}$ – a field, really – acting everywhere in the x direction at the surface of the liquid. For a cross-section perpendicular to the x-axis which we will take to have unitary area A, a virtual displacement δx [7] will generate a spacial volume change

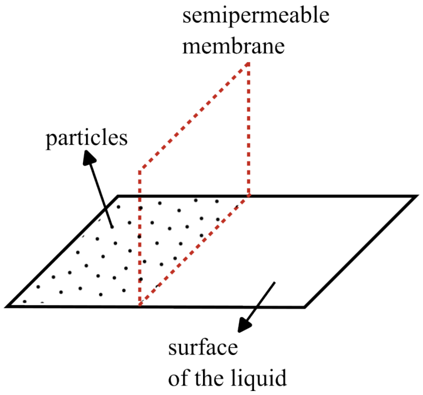

Figure 1.4: Diagram representing the particles suspended on the surface of a liquid.

of $\delta V = A\delta x$, at equilibrium

$$\delta F = \delta E - T\delta S = 0. \tag{1.21}$$

But, for a recipient of size L,

$$\delta E = \delta W = -\int_0^L \frac{N}{V^*} f \delta x dx \tag{1.22}$$

and for the entropy $dS = \frac{n_P R}{V^*} dV^*$, then

$$S = \int_{V^*} \frac{n_p R}{V^*} dV^* = \int_0^L \frac{n_p R}{V^*} (1 \cdot dx). \tag{1.23}$$

So, $\delta S = \int R\nu(x) \frac{\partial \delta x}{\partial x} dx$ and, by parts [4],

$$\delta S = -\frac{R}{N_A} \int_0^L \frac{\partial \nu}{\partial x} \delta x dx, \tag{1.24}$$

where $\nu / N_A = n_p / V^*$.

Thus, by equation (1.21),

$$\nu f - \underbrace{\frac{RT}{N_A} \frac{\partial \nu}{\partial x}}_{dP/dx} = 0. \tag{1.25}$$

For slow velocities like the ones we are dealing with, for a spherical particle of radius r, a force f of drag given by Stokes's law ($f = 6\pi k r v$) applies to a high degree of precision. Here k indicates the viscosity coefficient of the liquid. In this manner, we can interpret equation (1.25) as a diffusion of the particles with a force of resistance made by the fluid. On this basis, as Einstein concludes, the flux of particles through a unit of area per unit of time is given by $\frac{\nu f}{6\pi k r}$. Promptly we can write an expression for the coefficient of diffusion D first presented in section (1.2), i.e.

$$\frac{\nu f}{6\pi k r} - D \frac{\partial \nu}{\partial x} = 0, \tag{1.26}$$

with $D = \frac{RT}{N_A} \frac{1}{6\pi k r}$.

1.4.3 Diffusion

Because, as we have shown, the particles experience diffusion, their movement should obey a diffusion equation. Now we demand that: i) the collision of one particle does not depend on others and ii) each consecutive collision to be independent of the previous one. That being so, if we have N particles suspended on the surface of the volume V^* after some time τ each one of them will move of Δ_i in the x-axis [5]. The actual movement will depend on a probability distribution function $\phi(\Delta)$ and, as a result,

$$dN = N\phi(\Delta) d\Delta, \tag{1.27}$$

and, of course $\int_{-\infty}^{\infty} \phi(\Delta) d\Delta = 1$. Since no direction is privileged we will also impose that

$$\phi(\Delta) = \phi(-\Delta), \tag{1.28}$$

along with the assumption that $\nu(x,t)$ depends only on x and t. Since τ is very small (as well as Δ) it is possible to approximate $\nu(x, t+\tau)$ as

$$\nu(x, t+\tau) = \nu(x,t) + \frac{\partial \nu}{\partial t} \tau \tag{1.29}$$

also,

$$\nu(x+\Delta, t) = \nu(x,t) + \frac{\partial \nu}{\partial x} \Delta + \frac{\partial^2 \nu}{\partial x^2} \frac{\Delta^2}{2!} + \cdots \tag{1.30}$$

Equating equations (1.29) and (1.30), multiplying them by $\phi(\Delta)$ and integrating ($\int_{-\infty}^{\infty} d\Delta$) both sides yields,

$$\frac{\partial \nu}{\partial t} = D \frac{\partial^2 \nu}{\partial x^2}, \tag{1.31}$$

where it was used equation (1.28) and exploited the parity of the term of first-order on the integral. Equation (1.31) is known as the *diffusion equation* and its general solution is given by

$$\nu(x,t) = \frac{N}{\sqrt{4\pi D t}} \exp\Big\{ \Big(-\frac{x^2}{4Dt} \Big) \Big\}, \tag{1.32}$$

where it is assumed that it is possible to use a coordinate system with the origin at the center of mass of the set of all particles at $t = 0$. Therefore, the mean displacement squared is then given by equation (1.5), which astoundingly allows us to determine Avogadro's number,

$$N_A = \frac{RT}{3\pi \lambda_x^2 k r}, \tag{1.33}$$

a *universal* constant that ties the microscopic world with the huge scale we deal with every day. This could be done, and was done by Perrin, by careful observation of the movement of a couple of gamboge particles floating on water.

1.5 Conclusion

As it is clear from what we have seen until now, the Brownian motion is nothing more than a consequence of the atomic nature of matter. In showing that, Einstein was not only able to solidify the

---

[4] $\delta x(0) = \delta x(L) = 0$.

[5] A Δ_i for each particle i.

kinetic theory of heat but also provided a way of directly measuring Avogadro's number. His use of mostly thermodynamics – a highly empirical science – is an exemplary display of intuition and ingenuity in advancing, then, the still foggy view of atomic dynamics, and it is, without doubt, an important lesson for any aspiring scientist.

Bibliografia

[1] Einstein, A. & Brown, R. Investigations on the theory of the Brownian movement. (Dover Publ,1967)

[2] Nussenzveig, H. Curso de física básica. (Blucher,2008), OCLC: 457562460

[3] M. Jean Perrin, J. Atoms. (Constable,1916), http://archive.org/details/atoms00perrgoog

[4] Brown, H. & Irving, K. The size and weight of common allergenic pollens: An Investigation of Their Number Per Microgram and Size Distribution. *Allergy*. **28**, 132-137 (1973,7), https://onlinelibrary.wiley.com/doi/10.1111/j.1398-9995.1973.tb01319.x

[5] Karlin, S. & Taylor, H. A first course in stochastic processes. (Academic Press,1975)

[6] Strathmann, H. Ion-Exchange Membrane Separation Processes. (Elsevier B.V.,2004)

[7] Lemos, N. Mecânica analítica. (Editora Livraria da Física,2013), OCLC: 1402613971

[8] Maiocchi, R. The case of Brownian motion. *The British Journal For The History Of Science*. **23**, 257-283 (1990,9).

[9] AB, N. The Nobel Prize in Physics 1926. , https://www.nobelprize.org/prizes/physics/1926/summary/

2

From light to power: Thermodynamic insights into solar cells

Yosthyn M. A. Florez

Instituto de Física de São Carlos, Universidade de São Paulo, 13560-970 São Carlos, SP, Brazil

Abstract: Solar radiation is a reliable clean energy source, but its intermittent nature necessitates supplementary fossil fuel power, prompting extensive research. Developed in the 19th century, solar cells convert light energy into electrical current, and their theoretical understanding has evolved significantly, influenced by thermodynamics. This monograph explores the basic principles and equivalent circuit models of solar cells, evaluating key performance parameters such as maximum power and efficiency. It explores thermodynamics in photovoltaic conversion, focusing on efficiency limits and the integration of solar blackbody radiation. Additionally, various heat engine models for solar energy conversion, including the Carnot cycle and optical heat pumps, are analyzed for their efficiency in capturing and converting solar energy.

2.1 Introduction

Energy consumption profoundly influences our daily lives, making research into energy solutions is essential [1]. Among renewable energy technologies, solar photovoltaic (PV) cells are particularly noteworthy for their rapid advancement and promising future applications. As environmental concerns become more pressing, the importance of generating clean energy continues to grow. Although solar radiation is a reliable source of clean energy, its intermittent nature at specific locations means that PV systems often require supplementary power from fossil fuel sources. This challenge has been the focus of extensive research efforts [2].

A solar cell, also referred to as a photovoltaic cell, is a device that transforms light energy into electrical current. Although solar cells were first developed in the 19th century [3], the theoretical explanation of their functioning principles is still somewhat lacking. Emerging during the height of the industrial revolution, classical thermodynamics has extended beyond its original confines within the energy sector to become a fundamental pillar of science, influencing a wide array of scientific disciplines today. Therefore, it is not unexpected that thermodynamics has been employed to provide the theoretical framework required to advance even one of the most modern methods of energy conversion: photovoltaics.

The "Shockley paradox" was one of the first instances of thermodynamics being discussed in relation to solar cell operation [5]. Nonetheless, we will demonstrate that numerous concepts underlying the thermodynamic principles of solar cell functioning originate from a very earlier period. Systems for converting photochemical energy, such as biological photosynthesis and photoelectric devices, function by collecting a portion of the radiation occurring within a certain wavelength range. Photons with wavelengths longer than the cutoff wavelength are not employed by PV systems, and photon energies greater than the cutoff, or band-gap energy, are wasted as heat.

The incorporation of thermodynamics into the study of solar cells has been highlighted by several important turning points throughout history. This path, which starts with early theoretical frameworks and ends with contemporary experimental validations, illustrates ongoing efforts to efficiently harness solar energy. This monograph will explore the relationship between thermodynamics and our comprehension of solar cell operation, elaborating on the principles that govern energy conversion in photovoltaic systems.

2.2 Basic principles of a solar cell

The general structure of a solar cell consists of a thin layer of n-type material and a thicker layer of p-type material. The two separate layers are electrically neutral, and when brought together, an electric field is generated at the ‘p-n’ junction.

When light strikes the cell, the photons generate an electron-hole pair. The electric field at the junction separates them to prevent them from recombining, bringing the electrons to the ‘n’ region and the holes to the ‘p’ region. An external conductor connects the cell to a load, generating a flow of electrons from the ‘p’ zone to the ‘n’ zone [6].

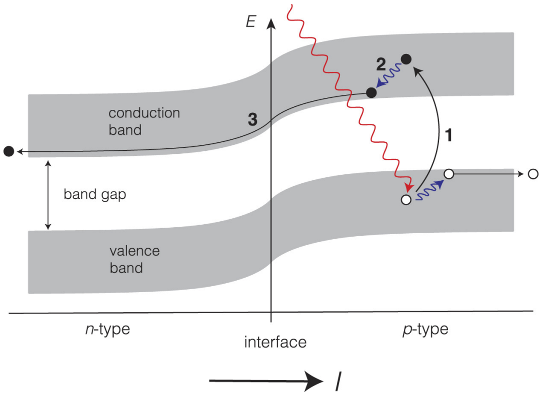

Figure 2.1: Procedures in the conventional textbook explanation of the solar energy effect: 1. In the semiconductor’s p-type phase, a photon is absorbed, creating a conducting pair (an electron and a hole). 2. The energy excess above the band gap is swiftly dissipated by the pair when they thermalize with the phonons in the lattice. 3. The potential difference across the interface drives the electron to the left, while the hole goes to the right, producing a voltage between the two terminals [6].

2.2.1 Equivalent circuit model

The typical representation of a working solar cell’s response is through an equivalent circuit model [7]. Figure 2.2 shows the equivalent circuit of an ideal solar cell, consisting of a current source (I_{PH}) responsible for the current generated by light under fixed solar radiation, a diode with current I_D that aids in rectifying the current, and the current I_{SH} flowing through the shunt resistance. Energy losses in the cell are depicted by series and parallel resistances. R_S (series resistance) includes all series resistances (contacts, metal-semiconductor contact, and the semiconductor itself) that impact cell performance. R_{SH} (shunt resistance) is linked to the diode’s leakage current, affecting operation in the current source region, along with a potential load resistance R_E from the external circuit.

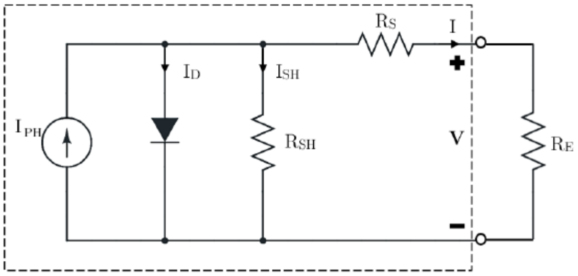

Figure 2.2: Equivalent circuit of a solar cell.

Through this equivalent circuit, the characteristic equation of a solar cell is deduced, which establishes a relationship between the parameters that define the current and the output potential.

$$I = I_{PH} - I_0(\exp^{\frac{qV_J}{nV_T}} - 1) - \frac{V + IR_S}{R_{SH}} \tag{2.1}$$

Where, I_0 is the reverse saturation current, n is the diode ideality factor, q is the elementary charge, and $V_T = \frac{kT}{q}$ is the thermal voltage (0.0259 volts at 298 K), where k is the Boltzmann constant and T is the temperature. This approach allows for the extraction of the values of these parameters based on their combined influence on the solar cell’s response.

2.2.2 Solar cells parameters

The main parameters used to evaluate the performance of solar cells are as follows: maximum power (P_{max}), which represents the maximum amount of energy generated; short-circuit current (I_{sc}), which reflects the maximum current produced; open-circuit potential (V_{oc}), which is the maximum potential obtained with no load; fill factor (FF), which indicates the efficiency of occupying the current-voltage curve; power conversion efficiency (PCE), which measures the ability to convert into useful energy; and external quantum efficiency (EQE), which evaluates the response at different wavelengths of incident light. Figure 2.3 shows the characteristic current-voltage curves of a solar cell both in the dark and under illumination, as well as the corresponding power curve.

$$I_{SC} \approx I_{PH} \tag{2.2}$$

$$J_{SC} = \int_{300nm}^{900nm} \phi(\lambda) EQE(\lambda) d\lambda \tag{2.3}$$

$$V_{OC} \approx \frac{nkT}{q} \ln\left(\frac{I_{PH}}{I_0} + 1\right) \tag{2.4}$$

$$FF = \frac{J_{mpp} * V_{mpp}}{V_{OC} * J_{SC}} \tag{2.5}$$

$$\eta = \frac{P_{max}}{P_{in}} = \frac{i_{mpp} V_{mpp}}{I_{in} A} = \frac{J_{SC} V_{OC} FF}{I_{in}} \tag{2.6}$$

$$EQE = \frac{\#electrons \;\; generated}{\#incident \;\; photons} \tag{2.7}$$

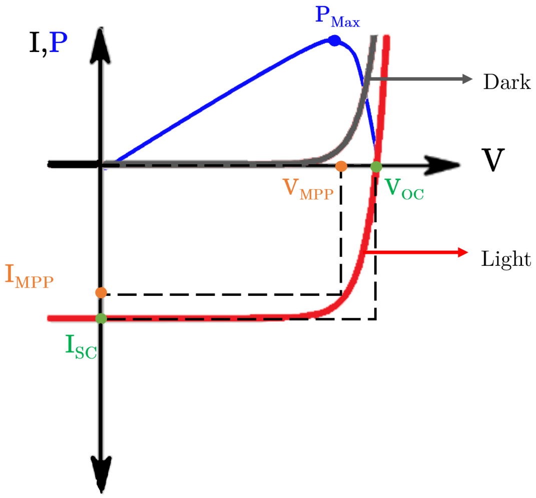

Figure 2.3: Current-Voltage and Power-Voltage characteristics curve of a solar cell: This graph illustrates the relationship between the current (I) and voltage (V), as well as the power (P) and voltage (V) in a solar cell.

2.3 Thermodynamics of photovoltaic conversion: Solar cell as a heat engine

Solar energy can be characterized by both its intensity and its spectral distribution. When sunlight hits a semiconductor with a bandgap (Eg), photons with energy below the bandgap are refracted and not absorbed. On the other hand, photons with energy higher than the bandgap have the ability to excite electron-hole pairs at different energy levels. After this excitation, the electron-hole pairs relax until they reach the bandgap energy before being collected by the contacts.

To consider an ideal scenario, let's imagine that all photons with energy higher than the bandgap are completely absorbed, and the semiconductor is so pure that there is no recombination of electron-hole pairs due to impurities. Simply put, the thermodynamic calculation can be considered if we assume that the sun emits monochromatic light, i.e. with a single frequency (ν). This light falls on a set of molecules, each with two energy levels, where $\hbar\omega = Eph = E2 - E1$ (according to Ref. [8]). For the real sun, the calculation will involve integrating the radiation from the solar blackbody, which will require solving some simple integrals.

2.3.1 Maximum thermodynamic efficiency of a two-Level solar cell

Here, we describe the basic energy conversion limitations when considering a solar cell as a "photon engine" that runs between the sun and the surrounding environment. We talk about the physics involved in a two-level group of atoms operating photovoltaically.

- **Idealized two-level system physics:** Imagine a group of two-level "atoms" that are immersed in a three-dimensional, isotropic photon field (the atoms are lit from all sides). We will consider discrete levels into mind; however, the same findings hold provided that the bandwidths are substantially lower than the photon energy. In this part, we will demonstrate that we could achieve or even surpass the Carnot efficiency, which is the maximum energy conversion in any thermodynamic engine, if we could connect these atoms to weak probes in order to collect the photogenerated electrons.

- **Two-level structure with a monochrome sun:** The Fermi-Dirac distribution (FD) usually governs the relative populations of atoms in the ground state E2 vs those in the excited states E1, given that the atoms stay in equilibrium with the surrounding phonons and photons.

$$f_i = \frac{1}{e^{(E_i - \mu_i)/K_B T_D} + 1} \tag{2.8}$$

where μ is the electrochemical potential associated with energy level i (1 or 2), k_B is the Boltzmann constant, and T_D is the absolute temperature of the two-level system. Keep in consideration that $(\mu_1 - \mu_2)_D$ does not always equal zero. The "device" in this case is denoted by the subscript "D". We consider just radiative recombination and exclude out any other non-radiative processes in order to get the basic limitations. The "up" or absorption transition is provided by

$$U(E_2 \rightarrow E_1) = \alpha f_2(1 - f_1)n_{ph} \tag{2.9}$$

whereas the "down" transition or emission is provided by

$$D(E_1 \rightarrow E_2) = \alpha f_1(1 - f_2)(n_{ph} + 1) \tag{2.10}$$

Here, α is a constant. The additional term of 1 on the right-hand side of the downward transition represents spontaneous emission. Moreover, n_{ph} is the Bose-Einstein (BE) distribution for isotropic photons, given by:

$$n_{ph}(T_S) = \frac{1}{e^{[(E_1-E_2)-(\mu_1-\mu_2)_s]/k_B T_S} - 1} \tag{2.11}$$

The form of equation 2.11 may seem unfamiliar, yet it can be easily derived. Consider the sun as an isolated box containing atoms and photons in equilibrium at the absolute temperature T_S. By equating equations 2.9 and 2.10 and using equation 2.8 as needed, we can solve for $n_{ph}(T_S)$. Although the sun is powered by internal nuclear reactions, measurements of the solar spectrum indicate that $(\mu_1 - \mu_2)_S \equiv \Delta\mu_S$ [9, 10]. We will use this assumption in the subsequent discussion.

For the two-level system maintained at temperature T_D [ruled by eq. 2.8] and lighted by photons from a source at temperature T_S [controlled by eq. 2.11], the absorption (U) must be balanced by emission (D) under a "open-circuit" condition—when electrons are not being taken from the system.

$$f_1(1 - f_2)(n_{ph} + 1) = f_2(1 - f_1)n_{ph} \tag{2.12}$$

Equation 2.13 is found by equations 2.11 and into it.

$$\frac{E_2 - \mu_2}{T_D} + \frac{E_1 - E_2}{T_S} = \frac{E_1 - \mu_1}{T_D} \tag{2.13}$$

or equivalently

$$qV_{OC} \equiv (\mu_1 - \mu_2)_D = (E_1 - E_2)\left[1 - \frac{T_D}{T_S}\right] \tag{2.14}$$

Therefore, V_{oc} represents the open-circuit voltage of the system, and q denotes the electron charge. Note the presence of the Carnot factor, which involves the ratio between the device temperature and the sun's temperature.

Now, if we connect a pair of electrodes to each atom—one electrode exchanging electrons exclusively with E_1 and the other with E_2 (see Fig.2.4)—and if the photon flux R from the sun is small, the energy input to the set of atoms is $(E_1 - E_2) \times N$. The maximum energy output is $\sim V_{oc} \times q \times N = (\mu_1 - \mu_2) \times N$. Thus, the efficiency η is given by:

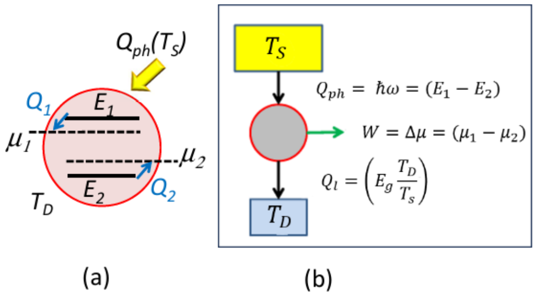

Figure 2.4: (a) Energy band diagram illustrating the 2-level system. (b) Energy flux balance diagram depicting a 'photon engine' [8].

$$\boxed{\eta = \frac{(\mu_1 - \mu_2)_D \times N}{(E_1 - E_2) \times N} = \left[1 - \frac{T_D}{T_S}\right]} \tag{2.15}$$

We assume that no additional losses are introduced by the probes used to extract the carriers. The input and output powers, which are used to derive the efficiency of the 2-level photovoltaic system [Eq.2.15], can be analogized to a Carnot *photon engine*.

2.4 Different solar energy conversion heat engines

This section explores different types of heat engines that have been considered at various times in the context of solar energy conversion, relating them to the concept of Carnot efficiency. Each of these engines proposes different approaches to maximizing efficiency in capturing and converting solar energy into usable forms of energy, using the fundamental principles of thermodynamics to optimize performance.

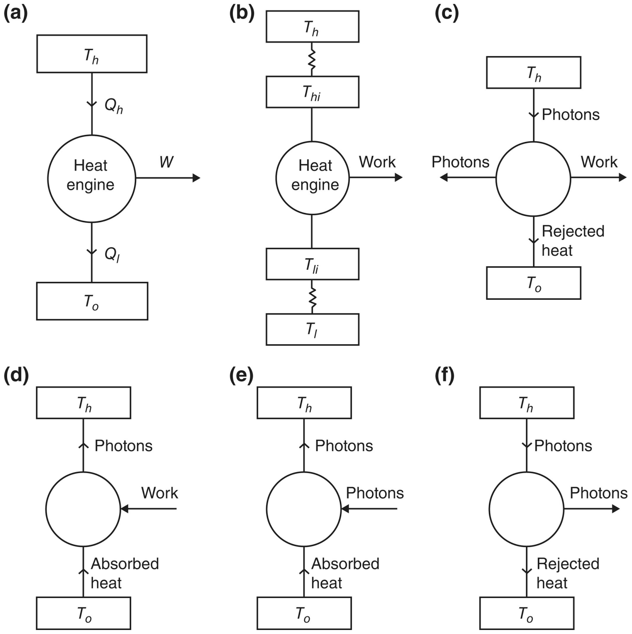

Figure 2.5: Various types of heat engines in solar energy conversion are depicted [4]: (a) Carnot cycle, with heat absorption at T_h and rejection at T_o; (b) endoreversible engine, operating between T_{hi} and T_{li}; (c) solar energy converter, absorbing photons at T_h, rejecting heat at T_o, and emitting photons while performing work; (d) optical heat pump, converting electrical input and low-grade heat at T_o into photon emission at T_h; (e) photoluminescence device model; (f) light-emitting device as a model for a solar cell.

Various types of heat engines have been contemplated over time within the realm of solar energy conversion. In the figure 2.5 a), we can see the initial point of departure in our discussion is a schematic representation of the Carnot cycle. Here, the engine absorbs heat Q_h from a high-temperature reservoir at T_h and releases heat Q_l into a low-temperature reservoir, consistently assumed in this paper to be at the ambient temperature T_o. Next, in the figure 2.5 b) schematic depiction of the endoreversible engine [11] shows heat exchange through jagged lines, operating between reservoirs at temperatures T_{hi} and T_{li}. Furthermore, figure. 2.5 c) The general concept of a solar energy converter [12] involves the absorption of photons as high-temperature heat at T_h, the rejection of heat at T_o, simultaneous photon emission, and work production. Moreover, figure. 2.5 d) Weinstein proposed an optical heat pump model where electrical input (considered as work) combined with low-grade heat at T_o results in photon emission equivalent to high-temperature heat at T_h [13]. Additionally, in the figure 2.5 e) Chukova considered an optical heat pump as a thermodynamic model for a photoluminescence device [14]. Finally, figure 2.5 f) A schematic of a light-emitting device, serving as a thermodynamic model for a solar cell [15].

- **The efficiency of a 2-level solar cell cannot be 100%.**

  What is the efficiency of the 2-level solar cell if the atoms are at room temperature (TD = 300 K) and the sun is a blackbody with TS = 6000 K?

  Solution:

$$\eta = \left[1 - \frac{300}{6000}\right] = 0.95 \approx 95\%$$

2.5 Conclusion

In conclusion, solar radiation, which can be represented as high-temperature heat, is effectively converted into useful work or electricity according to the laws of thermodynamics. This monograph discusses the fundamental limits of photovoltaic operation. Starting with a two-level model, we provide information on the basic operation of the solar cell and the loss mechanisms involved in ideal situations. Our analysis shows that an idealized two-level solar cell, working with isotropic light, can achieve a thermodynamic Carnot efficiency of 95%. This highlights the potential for high-efficiency solar energy conversion when ideal conditions are met and underscores the importance of continued research to minimize losses and improve the practical applications of solar technology.

Bibliografia

[1] Holechek, J. L. et al. *A global assessment: can renewable energy replace fossil fuels by 2050?* Sustainability, v. *14*, n. 8, p. 4792, 2022.

[2] Şen, Zekai. et al. *Solar energy in progress and future research trends. Progress in energy and combustion science*, vol. *30*, no 4, p. 367-416, 2004.

[3] Perlin, J. *Let it shine: the 6,000-year story of solar energy*. New World Library, 2002.

[4] Markvart, T. *From steam engine to solar cells: can thermodynamics guide the development of future generations of photovoltaics?*. Wiley Interdisciplinary Reviews: Energy and Environment, 2016, vol. *5*, no 5, p. 543-569

[5] Rose A. *Photovoltaic effect derived from the Carnot cycle*. J Appl Phys, v. *31* p. 1640, 1960.

[6] Alicki, Robert. et al. emphA thermodynamic cycle for the solar cell. Annals of Physics v. *378*, p. 71-87, 2017.

[7] Ćalasam, M. et. al *On the root mean square error (rmse) calculation for parameter estimation of photovoltaic models: A novel exact analytical solution based on lambert w function*. Energy Conversion and Management, v. *210*, p. 112716, 2020.

[8] Muhammad A. et. al.*Fundamentals of PV efficiency interpreted by a two-level model*. American Journal of Physics, 81(9):655–662, 2013.

[9] Robert F Pierret. *Advanced semiconductor fundamentals*. Prentice Hall, Upper Saddle River, N.J., 2003.

[10] F. Herrmann and P. Wurfel. *Light with nonzero chemical potential*. American Journal of Physics, 73(8):717, 2005.

[11] De Vos A. *Endoreversible Thermodynamics of SolarEnergy Conversion*. Oxford: Oxford UniversityPress; 1992.

[12] Landsberg PT, Tonge G. *Thermodynamics of the con-version of diluted radiation*. J Phys A ,12:551–562, 1979.

[13] Weinstein MA. *Thermodynamic limitation on theconversion of heat into light*. J Opt Soc Am,50:597–602, 1960.

[14] Chukova YP. *Thermodynamic limit of the lumines-cence efficiency*. Zh Eksp Teor Fiz Pisma Red,10:458–460, 1969.

[15] Markvart T. *Solar cell as a heat engine: energy-entropy analysis of photovoltaic conversion*. PhysStatus Solidi (a), 205:2752–2756, 2008.

[16] MARKVART, Tom.*From steam engine to solar cells: can thermodynamics guide the development of future generations of photovoltaics?* . Wiley Interdisciplinary Reviews: Energy and Environment, 2016, vol. 5, no 5, p. 543-569.